JOURNAL OF CATALYSIS 50, 353–363 (1977)

# Characterization of Enantioselective Hydrogenation Catalysts: Transient Electrochemical Oxidation of D-(+)-Tartaric Acid on Nickel

MIRIAM J. FISH AND DAVID F. OLLIS

*Department of Chemical Engineering, Princeton University, Princeton, New Jersey 08540*

Received December 31, 1976

The potential sweep method for measuring adsorbate coverages in liquid–solid systems has been modified for use with base metals such as nickel. Advantages and limitations of this method, as well as other techniques for determining liquid phase adsorption coverages, are discussed. The pH and temperature variation of D-(+)-tartaric acid adsorption on nickel is reported. The results are examined with relation to previous observations on the selectivity of nickel catalysts modified with D-(+)-tartaric acid in the enantioselective hydrogenation of $\beta$-keto esters. A simple model to describe the reported variation in hydrogenation optical yield vs pH of catalyst modification is presented.

## INTRODUCTION

Until recently, investigations of enantioselective hydrogenations by modified metal catalysts have been carried out in liquid phase reacting systems (*1–3*). Modification of the reduced or activated catalyst is achieved in an aqueous solution of an optically active modifying reagent. The modified catalyst is then recovered, washed, and immersed in an organic liquid phase containing the reactant. Subsequent catalytic hydrogenation leads to partially selective production of one product enantiomer form vs the nonselective racemic product mixture obtained with the unmodified catalyst. The most widely studied system has been the hydrogenation of $\beta$-keto esters by nickel powders or Raney nickel modified with the optically pure isomer of an amino or hydroxy acid. Modification with D-(+)-tartaric acid (TAR), in particular, gives relatively high optical yields.

To remove the complicating effects of the solvent, recent investigators have achieved both modification and reaction from the gas phase. Infrared studies of adsorbed modifier and reactant complexes (*4–7*) and kinetic data (*8*) have suggested structures for the adsorbed modifier and reactant–modifier complexes. While offering plausible explanations for both the occurrence and direction of enantioselectivity, they do not present quantitative results for the degree of enantioselectivity, which strongly depends on pH and temperature of modification (*1, 2*) and temperature (*9*) and solvent dielectric constant (*10*) in the reaction step. Quantitative measurements of modifier and reactant adsorption from the liquid phase as a function of modifying and reaction conditions, respectively, should provide insight on this point. With these considerations in mind, an electrochemical technique has been used to measure D-(+)-TAR adsorption onto nickel (Ni) from the liquid phase.

ISSN 0021-9517

### *Adsorption Measurements in Liquid–Solid Systems*

*Nonelectrochemical.* Adsorption coverages in liquid–solid can be obtained with only a few general procedures. Available data are limited, and interpretation is complicated by competitive solvent adsorption, solvent impurities, and ionic strength of pH effects.

The most familiar technique uses labeled adsorbates in a difference measurement between solution radioactivity levels before and after adsorption. As a difference method, the radiotracer technique suffers the disadvantage of requiring low liquid phase concentrations of adsorbate and/or large adsorbing surface areas in order to obtain measurable concentration changes. If a thin foil of the metal can be used, a direct adsorbate radioactivity measurement from the unwetted side of the foil is possible (*11–14*). In either a direct reading or difference radiotracer procedure, high background levels must be avoided.

Other difference techniques include quantitative spectrophotometric or titrimetric analyses of the solution before and after adsorption. These procedures are usually less sensitive than radiotracer detection.

Direct determinations have been made with destructive chemical analysis. After adsorption equilibrium is attained, the solid phase is recovered and subjected to a reagent which dissolves the solid without decomposing the adsorbate. Titrimetric or colorimetric analysis of the resulting solution gives a direct measurement of the amount adsorbed. Applied to a catalyst system, this technique requires large amounts of catalyst to obtain detectable levels of adsorbate, and the catalyst is destroyed at each measurement. Implicit is the assumption that no desorption occurs in the recovery step. The destructive procedure has been used previously to measure D-(+)-TAR adsorption on Ni (*8*).

*Electrochemical.* A final group of direct procedures involves programmed electrochemical oxidation of an adsorbate on an electrode. The total charge, $Q$, transferred in the oxidation can be measured and is proportional to the number of molecules oxidized, $N$:

$$Q = \frac{nFN}{N_0}, \tag{1}$$

where $F$ = Faraday's constant and $N_0$ = Avogadro's number.

For the enantioselective catalytic reactions of interest in this paper, the electrode is Ni and the adsorbate is D-(+)-TAR in aqueous solutions at various pH values and temperatures. An inorganic electrolyte is also present in solution to provide sufficient conductivity.

After suitable electrochemical pretreatment of the electrode to produce a reduced surface, adsorption is allowed to occur at controlled current or potential. The time to reach "equilibrium" is determined as the minimum adsorption time for which the measured charge of oxidation, $Q$, is the same as for any longer adsorption time. When adsorption "equilibrium" is reached, the electrode is subjected to a controlled current step (galvanostatic method), voltage step (potentiostatic method), or triangular voltage wave (potential sweep or potentiodynamic method). The resulting voltage (current) when current (voltage) is changed is monitored as a function of time. These traces are then analyzed to determine the total charge, $Q$. Further details are available in Refs. (*14–24*).

Adsorption of methanol (*17*, *18*), formic acid (*19*, *20*), ethylene and acetylene (*21*, *22*), and ethane (*21*, *23*) on platinum has been studied with one or more of these electrochemical techniques. A report on benzene adsorption on platinum has demonstrated the usefulness of each electrochemical method compared to the others and to radiotracer measurements (*14*).

Recently the potential sweep method has been applied to the determination of surface areas of platinum blacks by $H_2$ and CO adsorption and subsequent electrooxidation (*25, 26*); the results compared favorably with gas phase chemisorption measurements.

There are two unique advantages of the electrochemical techniques. Measurements are direct and nondestructive, and current levels corresponding to very low surface concentrations are easily monitored. Thus, low surface area electrodes can be studied, and the same electrode can be used for a large number of experiments. There is also the possibility, as yet not seriously examined, for measuring the simultaneous coverages of several adsorbates provided each oxidizes over a different potential range.

The extended application of electrochemical techniques must surmount two disadvantages. Experiments at low solute concentrations require caution to exclude low levels of other oxidizable impurities. Also, the methods must be adapted for use with base metals. Such alterations are now considered for the modifier–metal systems of major interest in enantioselective hydrogenations.

## EXPERIMENTAL METHODS

### *Nickel Electrodes*

The major difficulties with the application of electrochemical techniques to base rather than noble metals result from corrosion (dissolution) or passivation (rapid surface oxide or hydroxide formation) of such metals over a wide range of pH and applied voltage where oxidation of an organic adsorbate would typically occur. These regions are conveniently depicted on pH–voltage plots known as Pourbaix diagrams (*27*). A comparison of the nickel and platinum diagrams in Fig. 1 clearly indicates the much larger corrosion and passivation areas for the base metal in aqueous solutions.

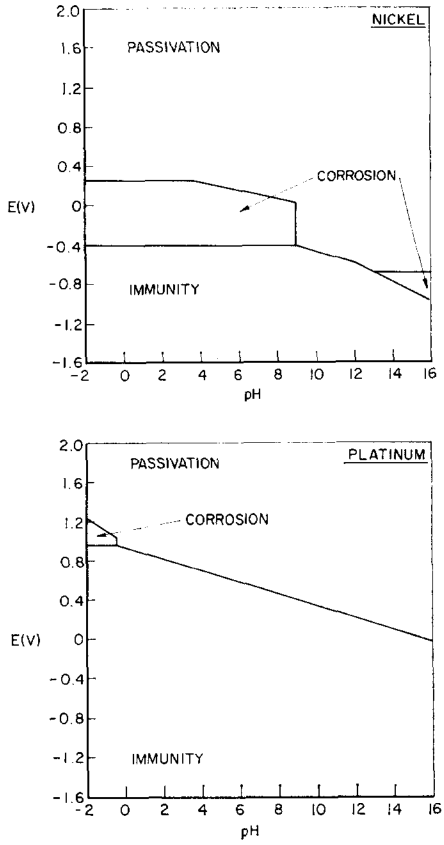

FIG. 1. Pourbaix diagrams for (top) nickel, (bottom) platinum, showing regions of immunity, passivation, and corrosion as functions of electrode potential and solution pH. The diagram for nickel is based on experimental results; the platinum diagram is based on thermodynamic calculations. [Graphs from Ref. (*27*); reproduced with the permission of Pergamon Press.]

For electrochemical measurement of surface coverages, the Pourbaix diagrams suggest that voltage rather than current be controlled in order to strictly avoid regions of dissolution. Of the two voltage control procedures, the potential sweep method offers a more readily interpreted result than the potentiostatic technique. By continuously changing the applied voltage over a particular range, the potential sweep procedure allows the voltage-dependent region of adsorbate oxidation to be distinguished from voltage-dependent regions of surface oxide or hydroxide formation.

Figure 2 illustrates this point with typical sweep curves for Ni in a blank solution and in 0.1 *M* TAR. In the potentiostatic method, however, a step to a sufficiently high voltage for complete oxidation of adsorbate may lead to desorption rather than oxidation of some adsorbate if the passivation reaction is fast compared to adsorbate oxidation, as might be expected for base metals. Because the voltage is now maintained constant, the two reactions cannot be distinguished.

From the Pourbaix diagram for Ni and some experimental observations, the following experimental procedure was found to give reasonable coverage measurements.

(i) The electrode is maintained at a reduction potential, $V_{red}$, lying in the range where adsorption is observed to be independent of the voltage. This insures complete surface reduction and eliminates the interference of hydrogen evolution with diffusion of adsorbate to the electrode (*12*). In these studies, $V_{red}$ is $-0.9$ V vs RHE and the reduction time, $t_{red}$, is 1–3 min, depending on solution temperature.

(ii) Adsorption is carried out at $V_{red}$ or open circuit until coverage becomes constant. For D-(+)-TAR adsorption on Ni at open circuit, an adsorption time, $t_{ads}$, of 10 min is sufficient. This adsorption time compares well with an earlier observation that optical yield in a hydrogenation reaction catalyzed by D-(+)-TAR-modified Raney nickel increased and then leveled out as modifier adsorption time reached 10–15 min (*1*). Obviously, the condition at open circuit parallels the original catalytic system. It can be argued, however, that adsorption at $V_{red}$ insures a reduced surface for comparison with previous gas and liquid phase studies. In the gas phase experiments the supported nickel catalyst was heated for 16 h at 350–400°C in a flowing $H_2$ atmosphere prior to modification (*4–6*). In most liquid phase studies the catalyst modified has been activated Raney nickel, which is also thought to be a reduced surface due to the presence of adsorbed hydrogen (*28*).

Because passivation is relatively rapid, modifier adsorption must occur from highly concentrated solutions. High modifier concentrations then allow successful competition of adsorption with surface oxide formation during open circuit adsorption at room temperature. Thus, measurements reflect the result of competitive reactions, not an isotherm. In this study, bulk concentrations below ~0.05 *M* TAR produced no measureable coverages; sweep results simultaneously indicated a completely passivated electrode. All values reported

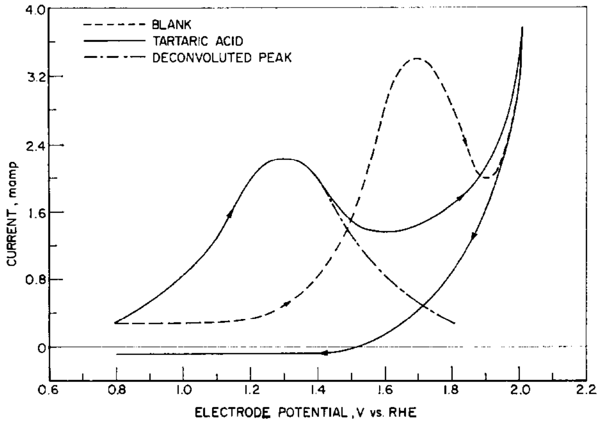

FIG. 2. Current traces obtained in blank and 0.1 *M* TAR. pH = 5.0; $T$ = 25°C; $V_{red} = V_{ads} = -0.9$ V vs RHE.

below refer to adsorption from 0.1 *M* (1.5%) D-(+)-TAR solutions.

This concentration limitation is consistent with the observation of extremely low optical yields in the hydrogenation reaction if the D-(+)-TAR concentration is below ~0.5% in the preliminary modification of Raney nickel (*29*). Above this level the optical yield increases sharply, reaching an upper plateau at modifier concentrations of 1.5–2.0% D-(+)-TAR. This implies a similar competition between adsorption and passivation as observed in the electrochemical system. Since open circuit potentials for Ni and some other base metals do fall in the passivation region, the term "adsorption isotherm" for liquid phase adsorption is not particularly meaningful for such metals.

(iii) Oxidation of the adsorbed species is carried out by a voltage step from $V_{\mathrm{red}}$ or $V_{\mathrm{open}}$ to $V_{\mathrm{initial}}$ and immediate initiation of a sweep. $V_{\mathrm{initial}}$ is chosen to bypass the corrosion region completely and to fall at the leading edge of the adsorbate oxidation peak. A lower choice of $V_{\mathrm{initial}}$ can allow some surface passivation accompanied by desorption of the adsorbate. This is evident for the D-(+)-TAR on Ni system from the smaller total currents of the TAR oxidation peak. A higher $V_{\mathrm{initial}}$ may not permit complete oxidation of adsorbate in the course of the sweep. Correspondingly, in the TAR–Ni studies, a smaller charge associated with the TAR oxidation peak is measured. The best value of $V_{\mathrm{initial}}$ was found to be +0.8 V vs RHE.

(iv) To determine the charge associated with adsorbate oxidation, the current curve is deconvoluted about the peak current assuming (a) a symmetrical waveform and (b) surface oxide formation occurring in the same voltage range as observed for the blank solution. The charge is obtained as the integral with respect to time of the deconvoluted current trace. Surface concentrations are calculated assuming complete oxidation, as validated for benzene on platinum (*14*). Less than complete TAR oxidation would increase the roughness factor correspondingly. TAR is completely oxidized in a 10-electron transfer half-reaction regardless of the degree of ionization of the adsorbed species.

$$C_4H_6O_6 + 2H_2O \rightarrow 4CO_2 + 10H^+ + 10e^-$$

$$C_4H_5O_6^- + 2H_2O \rightarrow 4CO_2 + 9H^+ + 10e^-$$

$$C_4H_4O_6^= + 2H_2O \rightarrow 4CO_2 + 8H^+ + 10e^-$$

In the TAR–Ni system the peak TAR oxidation current occurs at 1.0–1.3 V vs RHE, depending on temperature, while the leading edge of the oxide formation current falls in the same region, as seen in Fig. 2. In most cases the charge associated with oxide formation checks reasonably well (~25%) with that suggested by the amount of surface "protected" by adsorbed TAR at initiation of the sweep.

### *Apparatus*

Experiments were carried out in a standard three-compartment cell with the working electrode accessed to the reference electrode by a Luggin capillary. The working electrode was 99.9% pure 20-gauge Ni, Teflon-sheathed to expose 1.5 cm to the solution. A platinized platinum flag counter electrode and RHE reference electrode were separated from the working electrode compartment by stopcocks. Hydrogen to the reference electrode compartment and nitrogen for deoxygenating the cell solutions were passed through oxygen scrubbers and presaturators before entering the cell. A 0.05 *M* $Na_2SO_4$ electrolyte was used. All solutions were made with triple-distilled water and reagent grade chemicals; they were anodically and cathodically pre-electrolyzed for 24 h before use. Solutions were pH-adjusted with either dilute $H_2SO_4$ or NaOH. A heating tape and Therm-O-Watch laboratory controller maintained the cell solutions at the desired temperatures above ambient.

For each run a blank current (without adsorbate in solution) was determined along with an adsorbate trace at the desired pH and temperature. Before each measurement the solution was deoxygenated by bubbling $N_2$ through the cell for 30 min.

Potential control was maintained with a Princeton Applied Research (PAR) 173 potentiostat. The dual-channel potentiostatic control of this instrument required no special circuitry to achieve the potential step to $V_{\text{initial}}$ described in the previous section. The potential sweep was controlled with a PAR 175 voltage programmer coupled to the potentiostat. All current vs voltage traces were recorded on a Tektronix D11 storage oscilloscope with Polaroid photographs providing permanent records of the result. A sweep rate of 0.5 V/sec proved sufficient to avoid either bulk liquid film diffusional effects or intrinsic kinetic limitations of the oxidation reaction (*14*).

## RESULTS AND DISCUSSION

### *Surface Area Estimate*

Figure 3a is the current trace obtained when the Ni electrode in the blank solution is stepped from $V_{\text{red}}$ to $V_{\text{initial}}$ and then continuously subjected to multiple sweeps between $V_{\text{initial}}$ and $V_{\max}$, as illustrated in Fig. 3b. The upper curve (solid) is obtained on the first sweep, and the lower one (broken) on the second and all subsequent sweeps. Nearly the same set of curves is obtained over the entire pH (3.0–7.0) and temperature (25–80°C) ranges investigated. The curves can be used to estimate surface area if it is assumed that during the first sweep all reduced surface atoms are oxidized to a single surface oxide. Since all subsequent peaks are identical, passivation is complete during the first sweep. The difference between the areas under the two curves is then a measure of the charge required for oxide formation. Assuming a particular oxide stoichiometry and no multilayer oxide formation gives an estimate of the original reduced surface area. Reproducibility of the bare surface sweeps was typically within 5% of the mean.

In basic solutions in the potential range $V_{\text{initial}}$ to $V_{\max}$, the passivated layer is generally characterized as the oxide–hydroxide NiOOH (*30*). However, the present studies were made in neutral to acidic pH where $NiO_2$ is the thermodynamically favored compound (*27*). It is assumed here to be formed in the four-

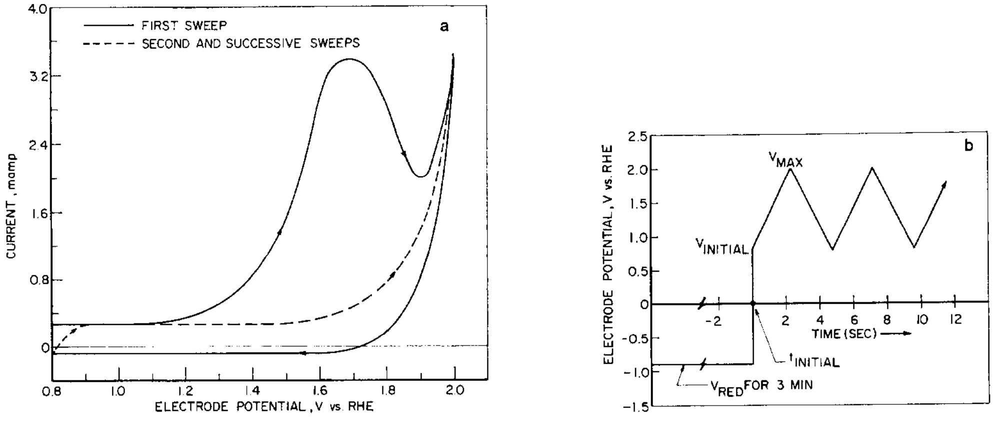

FIG. 3. (a) Current trace obtained when reduced nickel electrode was subjected to voltage program in Fig. 3b. (b) Electrode potential as function of time for traces obtained in Fig. 3a. Sweep rate = 0.5 V/sec.

electron transfer half-reaction:

$$Ni + 2H_2O \rightarrow NiO_2 + 4H^+ + 4e^-.$$

Depending on the crystal plane exposed, the surface area of the electrode can be calculated. The results for the three low index faces are presented in Table 1 based on the entire surface being composed of one face. The actual surface area will probably fall within the range of these values. For convenience, all D-(+)-TAR surface concentrations reported are based on the (111) surface area.

### *TAR Adsorption on Ni*

Figures 5 and 8 present measured TAR coverages as a function of solution pH and temperature, respectively. The fractional coverages are based on an assumed maximum surface concentration of D-(+)-TAR on Ni of $8.83 \times 10^{-10}$ mol/cm$^2$ ($5.3 \times 10^{14}$ molecules/cm$^2$). This value results from the assumption of carboxylate formation between a TAR anion and surface Ni atom (Fig. 4) as suggested from infrared spectra of D-(+)-TAR adsorbed on silica-supported Ni (*7*). By positioning three-dimensional hard sphere models of TAR anions on a two-dimensional scale model of each of the three low index planes, it appears that an average of 3–3.5 surface atoms are blocked per TAR molecule adsorbed (Table 1). One is directly involved in the bonding, and the others result from the partial or total blockage of neighboring atoms by the molecule extending out from the surface. Association of one TAR molecule with 3.5 surface Ni atoms leads directly to the stated value for maximum surface concentration on the (111) plane.

TABLE 1

Surface Area Estimate of Nickel Electrode

| Crystal face | Area/metal atom[a] (Å$^2$) | Total area[b] (cm$^2$) | Roughness factor[c] | Surface atoms/TAR molecule adsorbed |
|---|---|---|---|---|
| (111) | 5.378 | 2.11 | 5.6 | 3.5 |
| (100) | 6.210 | 2.44 | 6.4 | 3.5 |
| (110) | 8.782 | 3.45 | 9.1 | 3 |

[a] Based on Pauling radius for nickel = 1.246 Å (*31*).

[b] $Q$ (surface oxidation) = $2.516 \times 10^{-3}$ C.

[c] Apparent surface area = 0.38 cm$^2$.

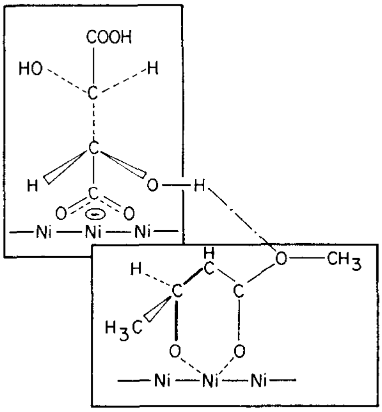

FIG. 4. Proposed interaction between adsorbed D-(+)-tartaric acid and adsorbed methyl acetoacetate. [Graph from Ref. (*6*)].

Another estimate of maximum surface coverage can be obtained by assuming that TAR adsorption on Ni occurs with rearrangement of the surface Ni atoms to produce a surface layer with properties of a bulk nickel tartrate salt. Several possible stoichiometries for these salts are: $NiC_4H_4O_6$, $NiC_4H_4O_6 \cdot xH_2O$ ($x$ = 3, 2.5, 1), and $Ni(C_4H_5O_6)_2$ (*32*). Lack of crystal structure information prevents evaluation of maximum surface concentration by this approach.

All electrochemically measured fractional coverages of D-(+)-TAR based on the blockage of surface atoms correspond to a monolayer or less, as expected if adsorption involves carboxylate formation. A previous study indicates that all TAR-modified catalysts display some catalytic, but not necessarily optically selective, activity for the hydrogenation reaction (*29*). Thus multilayer TAR adsorption is improbable since there must always be reactant adsorp-

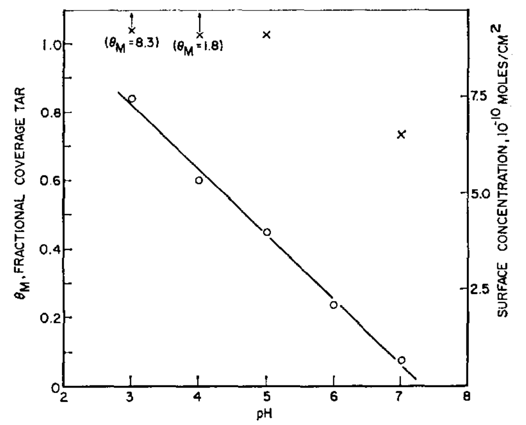

FIG. 5. pH Dependence of TAR adsorption on nickel. (○) This study: $T = 25°C$, $V_{ads} = V_{open}$; (×) Yasumori *et al.* (*8*): $T = 0°C$. (Data reprinted with permission from Elsevier Scientific Publishing Co.)

tion sites available. It therefore appears unreasonable that both acid groups of an adsorbed TAR molecule are bound to the surface, as postulated elsewhere (*7*). By reasoning as above, dicarboxylate formation would block about nine surface atoms per molecule adsorbed. The corresponding maximum surface concentration for the (111) plane is $3.43 \times 10^{-10}$ mol/cm$^2$ ($2.07 \times 10^{14}$ molecules/cm$^2$). Fractional coverages referred to this value are greater than one, hence dicarboxylate is doubtful.

In Figure 5 the electrochemically measured coverage dependence vs pH is compared with an earlier result in which TAR coverage was determined by destructive assay (*8*). Both sets of data show that the fractional coverage of TAR continuously increases as the adsorption pH decreases. The previous results imply multilayer coverage below pH 5.0. This is unlikely according to the arguments above.

Figure 6 shows the influence of pH of the modification step on the optical yield reported for the hydrogenation of methyl acetoacetate with Ni catalysts modified by D-(+)-TAR at 0°C. (The curves in Fig. 6 are the least-squares fit of Eq. (9) below.) The optical yield clearly exhibits a maximum with pH corresponding to an intermediate coverage of modifier (Fig. 5).

Klabunovskii (*3*) earlier suggested that both optically selective and optically nonselective reactant adsorption sites may exist on the surface. Denoting these by $S$ or $OS$ and $NS$, respectively, we now develop a simple model which rationalizes the existence of the optical yield maximum. At $NS$ sites both product enantiomers (+, −) are produced in equal amounts at a rate proportional to the total number of available adsorption sites:

$$r_{+,NS} = r_{-,NS} = \tfrac{1}{2}k(1 - \theta_M)^{y_{NS}} C_H^a C_R^b, \qquad (2)$$

where + = predominant product stereoisomer; − = other enantiomer form; $\theta_M$ = fractional coverage of modifier; $C_H$ = hydrogen concentration; $C_R$ = reactant (e.g., methyl acetoacetate) concentration; $y_{NS}$ = number of TAR adsorption sites in the reactant site, and $a$ and $b$ = reaction orders at $NS$ sites. At $OS$ sites the "+"

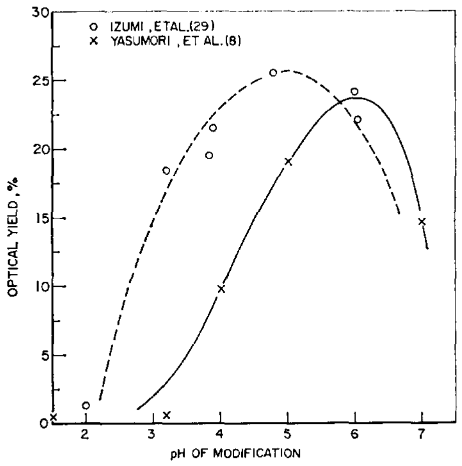

FIG. 6. Dependence of optical yield on pH of modification for the hydrogenation of methyl acetoacetate with Raney nickel modified by D-(+)-tartaric acid. Lines drawn through the data are the predictions of the proposed model [Eq. (9)] with the parameters in Table 2. [Data from Ref. (*8*) and (*29*); reprinted with permission from Elsevier Scientific Publishing Co. and The Chemical Society of Japan, respectively.

isomer is presumed to be produced exclusively and at a rate dependent on both *OS* adsorption sites available to the reactant and the neighboring presence of the modifier:

$$r_{+,OS} = k_{+}\theta_M{}^x(1 - \theta_M)^{y_{OS}}C_H{}^cC_R{}^d, \quad (3)$$

where $c$ and $d$ = reaction orders at *OS* sites, $x$ = number of modifier molecules in active site, and $y_{OS}$ is the corresponding analog of $y_{NS}$.

Reaction orders in both hydrogen and $\beta$-keto ester are about the same for reaction on modified and unmodified nickel catalysts (*8*); i.e., $a = c$ and $b = d$. Letting $p$ = optical yield and $S_p$ = optical isomer selectivity, the following relationships for these variables are obtained:

$$S_p = C_+/C_- \quad (4)$$

$$= r_+/r_- \quad (5)$$

$$= 1 + 2(k_+/k)\theta_M{}^x(1 - \theta_M)^{\Delta y}, \quad (6)$$

where $C_+$, and $C_-$ = concentrations of "+" and "−" enantiomers, respectively, and $\Delta y = y_{OS} - y_{NS}$.

$$p = [\alpha]_D/[\alpha]_D{}^0 \quad (7)$$

$$= (S_p - 1)/(S_p + 1) \quad (8)$$

$$= \frac{(k_+/k)\theta_M{}^x(1 - \theta_M)^{\Delta y}}{1 + (k_+/k)\theta_M{}^x(1 - \theta_M)^{\Delta y}}, \quad (9)$$

where $[\alpha]_D$ = optical rotation of the product and $[\alpha]_D{}^0$ = optical rotation of pure enantiomer. Equation (9) exhibits a maximum only for $x, \Delta y < 0$ or $x, \Delta y > 0$. Hydrogen bonding between reactant and modifier molecules (*6*–*8*) implies $x > 0$; for the proposed one-to-one interaction between reactant and modifier molecules (*6*) shown in Fig. 4, $x = 1$. A least-squares fit of Eq. (9) (with $x = 1.0$) to the data in Fig. 6 gives the results presented in Table 2. Evaluation of the model with the data of Yasumori *et al.* (*8*) (solid line in Fig. 6) is difficult due to the relatively small number of points, particularly in the vicinity of the predicted maximum. On the other hand, the results of Izumi *et al.* (*29*) are well described by Eq. (9) (dashed line in Fig. 6). The maximum in optical yield at a pH of 5.0 predicted for these data also corresponds to the highest value reported by Yasumori *et al.*, although the latter results are best fit with the maximum located at a pH of 6.0.

TABLE 2

Parameters Determined for Eq. (9)

| Source of optical yield data | pH at $p_{max}$ | $\theta_M$ at $p_{max}$ (Fig. 5) | $\Delta y = y_{OS} - y_{NS}$ | $k_+/k$ |
|---|---|---|---|---|
| Izumi *et al.* (*29*) | 5.0 | 0.45 | 1.2 | 1.57 |
| Yasumori *et al.* (*8*) | 6.0 | 0.26 | 2.85 | 2.81 |

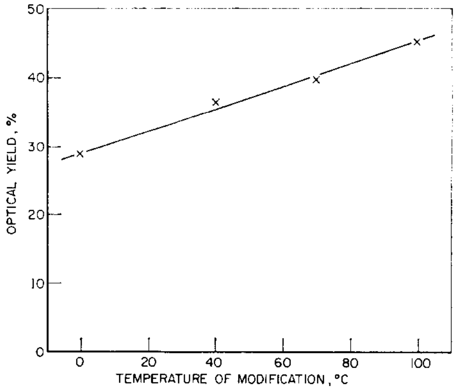

FIG. 7. Dependence of optical yield on temperature of modification for the hydrogenation of methyl acetoacetate with Raney nickel modified by D-(+)-tartaric acid (pH = 5.0). [Data from Ref. (*1*); reprinted with permission from The Chemical Society of Japan.]

In both cases $\Delta y = y_{OS} - y_{NS}$ is greater than zero. Values of $y_{OS}$ or $y_{NS}$ other than 1 arise if more or less surface area is required for reactant vs modifier adsorption. The requirement of $y_{OS} > y_{NS}$ for a maximum in optical yield vs pH of modification (i.e., modifier coverage) suggests that a reactant molecule adsorbed on an *OS* site requires more metal surface area than one adsorbed at an *NS* site. In both cases, also, $(k_+/k)$ is greater than 1, or the rate constant at *OS* sites is greater than that at *NS* sites.

The model is consistent with previous observations: namely that the optical yield

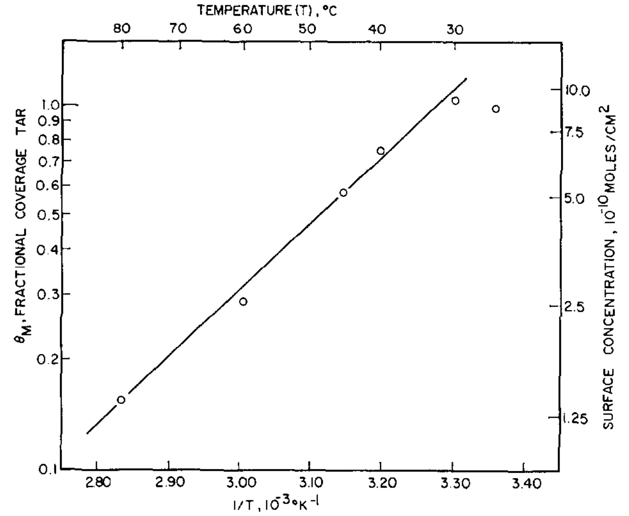

FIG. 8. Temperature dependence of TAR adsorption on nickel. $V_{ads} = V_{open}$.

is zero on an unmodified catalyst ($r_{OS} = 0$ and $S_p = 1$) and that it exhibits a maximum at intermediate modifier coverage. The model further implies that with increasing modifier coverage, the overall rate, $r = r_{OS} + r_{NS}$, should decrease. This corresponds to a statement made elsewhere, but without supporting data (*3*), that as the optical yield increased, the overall rate decreased.[1]

The dependence of TAR coverage on pH (Fig. 5) may be the result of competition between TAR adsorption rate and surface passivation rate. The half reaction cited earlier which yields $NiO_2$ also produces acid ($H^+$); it is not unreasonable that this passivation reaction might be more rapid in neutral versus acid medium. Qualitatively, the measured TAR coverage would increase with more acidic pH, as indicated in Fig. 5.

As the temperature of modification increases from 0 to 100°C at constant modification pH of 5.0 for D-(+)-TAR-modified Raney Ni, the corresponding optical yield obtained in the hydrogenation of methyl acetoacetate has been observed to increase from 20 to 45% (*1*), as shown in Fig. 7. Electrochemical measurements of adsorption at $V_{ads} = V_{red}$ indicate a decrease in TAR coverage as the temperature rises, as seen in Fig. 8. Similar experiments at $V_{ads} = V_{open}$ show no detectable coverage at temperatures above ambient probably because the passivation rate at the electrode becomes much greater than the TAR adsorption or oxidation rate. Since measurements were not made at $V_{open}$, comparison of these data with the previous result at pH = 5.0 (Fig. 5) is not appropriate.

The temperature dependence of the measured TAR coverage may be dominated by

---

[1] The simple model of this paper assumes that each modifier molecule is independent of others. Alternatively, a more complicated model could be envisaged, as follows: (i) Adsorbing tartrate may form islands by a cooperative interaction, analogous to the surface anhydrides proposed for the simpler carboxylic acids (formic or acetic) adsorbed from the vapor phase on Ni(110) surfaces (Madix, R. J., *et al.*, *Surface Sci.* **42**, 329 (1974); **46**, 473 (1974); **54**, 6 (1976). (ii) In such close packed islands, the optically selective sites would likely occur at the perimeter of each island. (iii) If the number of such islands per square centimeter is independent of coverage, $\theta_{TAR}$, then the ratio of perimeter (*OS*) to uncovered surface (*NS*) will exhibit a maximum as $\theta_{TAR}$ increases from 0 to unity. As many more assumptions are implicit in this model, and as the generality with which such islands form on other nickel planes, and in liquid–solid systems, is unknown, it is not further pursued here.

the activation energy differences between the surface passivation reaction and TAR adsorption rate. While the reaction leading to a nickel surface "carboxylate" is favorable, it is known that nickel reacts with water to produce oxides with large heats of formation (*27*). The affinity of water for nickel can also rationalize the large drop in optical yield (35 to 1%) obtained in the hydrogenation of methyl acetoacetate by D-(+)-TAR-modified Raney Ni when $H_2O$ is present in the reaction vessel (*33*).

In summary, the results of the potential sweep method for measuring the surface coverage of D-(+)-tartaric acid on nickel appear very reasonable. Measured coverages correspond to a monolayer or less, as expected from independent observations of catalytic activity of Raney nickel modified with D-(+)-tartaric acid (*29*). The increase in TAR adsorption with decreasing solution pH observed in this and earlier studies (*1*, *8*) can be incorporated in a simple model which agrees with the reported maximum in optical yield for the hydrogenation reaction as a function of modifying pH.

## ACKNOWLEDGMENTS

The authors gratefully acknowledge support of the American Chemical Society and National Science Foundation. One of the authors (M.J.F.) expresses her appreciation to the American Association of University Women for fellowship support.

## REFERENCES

*1.* Tatsumi, S., *Bull. Chem. Soc. Japan* **41**, 408 (1968).
*2.* Izumi, Y., *Angew. Chem., Int. Ed.* **10**, 871 (1971).
*3.* Klabunovskii, E. I., *Russ. J. Phys. Chem.* **47**, 765 (1973).
*4.* Groenewegen, J. A., and Sachtler, W. M. H., *J. Catal.* **27**, 369 (1972).
*5.* Groenewegen, J. A., and Sachtler, W. M. H., *J. Catal.* **33**, 176 (1974).
*6.* Groenewegen, J. A., and Sachtler, W. M. H., *J. Catal.* **38**, 501 (1975).
*7.* Groenewegen, J. A., and Sachtler, W. M. H., *in* "Sixth Congress on Catalysis." Paper B40, London (7/76).
*8.* Yasumori, I., Inoue, Y., and Okabe, K., *in* Proceedings, International Symposium on the Relations between Heterogeneous and Homogeneous Catalytic Phenomena, 1974, pp. 41–52. Elsevier, Amsterdam, 1975.
*9.* Harada, T., *et al.*, *in* "Sixth Congress on Catalysis." Paper B41, London (7/76).
*10.* Lipgart, E. N., *et al.*, *Kinet. Katal.* **12**, 1320 (1970).
*11.* Green, M., *et al.*, *Rev. Sci. Instrum.* **33**, 18 (1962).
*12.* Bockris, J. O'M., and Swinkels, D. A. J., *J. Electrochem. Soc.* **111**, 736 (1964).
*13.* Bockris, J. O'M., and Swinkels, D. A. J., *J. Electrochem. Soc.* **111**, 743 (1964).
*14.* Gileadi, E., *et al.*, *Electrochim. Acta* **13**, 1915 (1968).
*15.* Bockris, J. O'M., and Reddy, A. K. N., "Modern Electrochemistry II," pp. 1029–1035. Plenum Press, New York, 1970.
*16.* Bockris, J. O'M., and Srinivasan, S., "Fuel Cells," pp. 471–481. McGraw-Hill, New York, 1969.
*17.* Breiter, M. W., and Gilman, S., *J. Electrochem. Soc.* **109**, 622 (1962).
*18.* Biegler, T., *Austr. J. Chem.* **22**, 1583 (1969).
*19.* Johnson, P. R., and Kuhn, A. T., *J. Electrochem. Soc.* **112**, 599 (1965).
*20.* Breiter, M. W., *Electrochim. Acta* **8**, 447 (1963).
*21.* Gilman, S., *J. Electrochem. Soc.* **113**, 1036 (1966).
*22.* Gilman, S., *Trans. Farad. Soc.* **62**, 466 (1966).
*23.* Niedrach, L. W., *et al.*, *J. Electrochem. Soc.* **112**, 1161 (1965).
*24.* Icenhower, D. E., *et al.*, *J. Electrochem. Soc.*, **117** 1500 (1970).
*25.* Stonehart, P., and Zucks, P. A., *Electrochim. Acta* **17**, 2333 (1972).
*26.* Bett, J., Kinoshita, K., Routsis, K., and Stonehart, P., *J. Catal.* **29**, 160 (1973).
*27.* Pourbaix, M., "Atlas of Electrochemical Equilibria," pp. 330–342, 381. Pergamon Press, Oxford, 1962.
*28.* Fouilloux, P., Martin, G. A., Renouprez, A. J., Moraweck, B., Imelik, B., and Prettre, M., *J. Catal.* **25**, 212 (1972).
*29.* Izumi, Y., *et al.*, *Bull. Chem. Soc. Japan* **36**, 155 (1963).
*30.* Weininger, J. L., and Breiter, M. W., *J. Electrochem. Soc.* **110**, 484 (1963).
*31.* Pauling, L., "The Nature of the Chemical Bond," (3rd ed.), p. 410. Cornell University Press, New York, 1960.
*32.* "Gmelin's Handbuch der Anorganischer Chemie, Nickel 57," Teil B, Lfg 3, pp. 885–890. Verlag Chemie, 1966.
*33.* Ninomiya, T., *Bull. Chem. Soc. Japan* **45**, 2545 (1972).